

ANALYSIS AND TESTS OF IMPACT DAMAGED SYMMETRIC AND BALANCED LAMINATES

Markus Wallin and Olli Saarela
Aalto University, School of Science and Technology
Department of Applied Mechanics

Keywords: *compression after impact, balanced laminate, failure strength*

Abstract

The damage tolerant design of aircraft structures is typically based on using strain limits in the structural design process. These strain limits are typically obtained in the coupon level using compression after impact test method (CAI). In CAI test the impact damaged laminate is subjected to a uniaxial compression loading using a test fixture that prevents the global buckling of the specimen.

An analysis method to predict the CAI strength of laminates was developed [1-2]. The method is based on analysis of the equivalent hole and the compression strength of the 0° layers. The analysis method can provide a good estimate for both notched and impact damaged laminates with various fiber orientations [3].

The main limitation for both CAI test and the analysis method is the uniaxial loading. In order to use the analysis method during the structural design and to estimate the damage tolerance of actual structures the method should be expanded to cover also multiaxial stress state.

The existing CAI test arrangements can be used to simulate multiaxial loading of the laminates. This is done by using laminate lay-ups that are symmetric and balanced but does not include any 0° layers. Although the laminate is loaded uniaxially all layers are in multiaxial stress state.

As a final conclusion the applicability of the analysis method to estimate multiaxial strength of composite laminates is obtained. In addition, the damage resistance and impact behavior of laminates with untypical layer orientations is investigated.

1 Introduction

The residual strength of impact damaged laminates is typically defined using compression after impact (CAI) test standard that is based on uniaxial compression loading. Analysis methods are developed to model the behavior of CAI specimens and they are found to work well. In practice the composite structures are in multiaxial loading conditions. Therefore, the applicability of the analysis methods is very limited

The analysis of the residual strength of the impact damaged composite structures requires that the analysis method takes into account the arbitrary in-plane loading conditions. General composite analysis software such as ESAComp include notched laminate analysis module. These analysis methods are typically based on point stress analysis and on the use of characteristic distance. Point stress analysis is possible to fit into a specific test data but is not necessarily applicable to other laminate lay-ups, notch geometries or loading conditions.

This paper presents an analysis method that enables the residual strength estimation using arbitrary in-plane loading. The work is based on existing analysis methods which are combined to produce more general analysis method for impact damaged laminates. The applicability of the analysis method is first compared to previous test results of quasi-isotropic notched laminates. Additional tests are performed using laminates with different lay-ups. These laminate lay-ups include balanced laminates without any 0° plies. Although, the tests are performed in uniaxial external compression loading all plies are in multiaxial stress state. This allows the use

of existing CAI test arrangements. The results obtained from these tests provide a valuable tool for multi-axial strength analysis of impact damaged composite laminates.

2 Analysis Method

In the previous paper [3] the analysis method used was developed for uniaxial loading of notched laminates. The analysis method was originally developed in [1] and [2]. The purpose of this research was to expand the analysis method in order to be able to use that with multi-axial loading cases in the future. In addition, the previous analysis method was based on maximum stress criterion. In this paper, several failure criteria including fully interactive criteria are used.

Although in this study the external loading used is uniaxial the need for new analysis method was considered necessary. In case of balanced laminates without 0° plies the failure does not necessarily occur at 90° angle with respect to the external loading. Therefore, the ability to analyze stresses with arbitrary angle around the notch was necessary.

The new analysis method is based on same equations which are used in ESAComp software. The main difference is that in ESAComp the analysis is based on point stress method whereas in this study the analysis is based on average stress method. However, the general stress solution is the same for both cases. The more detailed derivation of the equations is presented in [4]. In this paper only the final results are shown.

2.1 Analysis of Notched Laminate

The analysis method is based on an elliptical hole as shown in Fig. 1. In this paper the same notation is used as in ESAComp and it is different than in previous paper as well as in typical publications. In this case, the laminate x -axis is the same as the 0° direction of the laminate.

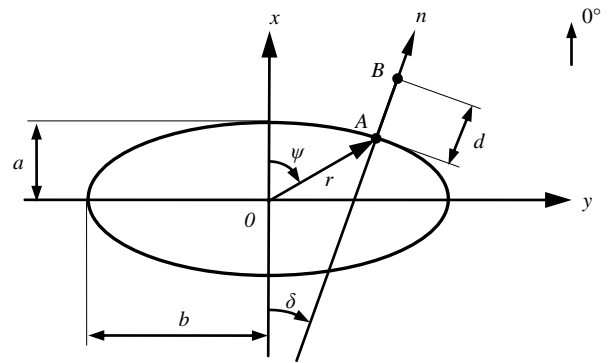


Fig. 1. Coordinates and notation of the elliptical hole

The stresses are calculated along the characteristic distance d from the edge of the hole i.e. between points A and B . The characteristic distance is the distance normal to the hole edge. A special case is the round hole where $a = b$ and angles $\psi = \delta$.

The distance of the hole edge from the origin is:

$$r = \frac{ab}{\sqrt{a^2 \sin^2 \psi + b^2 \cos^2 \psi}} \quad (1)$$

and the angles ψ and δ have the relation.

$$\delta = \tan^{-1} \left[\left(\frac{a}{b} \right)^2 \tan \psi \right] \quad (2)$$

2.2 Laminate Stresses

The derivation of the equations is summarized in [4]. The actual work is based on [5] and [6] among others. This paper presents only the final equations.

Let's consider an elliptical hole in laminate in arbitrary in-plane loading case $(\sigma_x^\infty, \sigma_y^\infty, \tau_{xy}^\infty)$ as shown in Fig. 2.

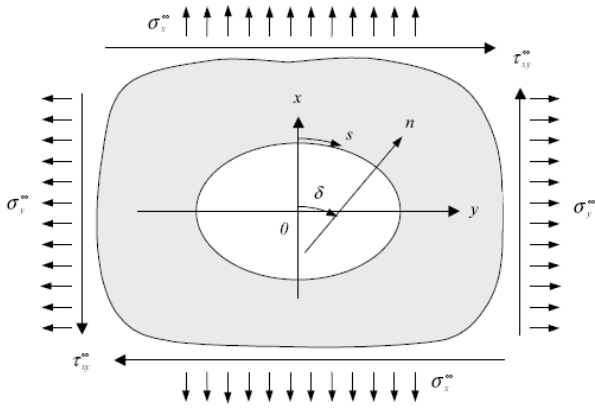


Fig. 2. Elliptical notch under in-plane loading [4]

The case in Fig. 2 can be analyzed using the principle of superposition by combining two cases according to the Fig 3. In case 3b the additional loading along the edge \hat{X}_n, \hat{Y}_n is defined in such way that the effect of notch vanishes i.e. the case 3b represents external loading. Therefore, the stresses in notched laminate, designated with superscript 0 are obtained from equation:

$$\{\sigma^0\}_{xy} = \{\sigma^\infty\}_{xy} + \{\sigma\}_{xy} \quad (3)$$

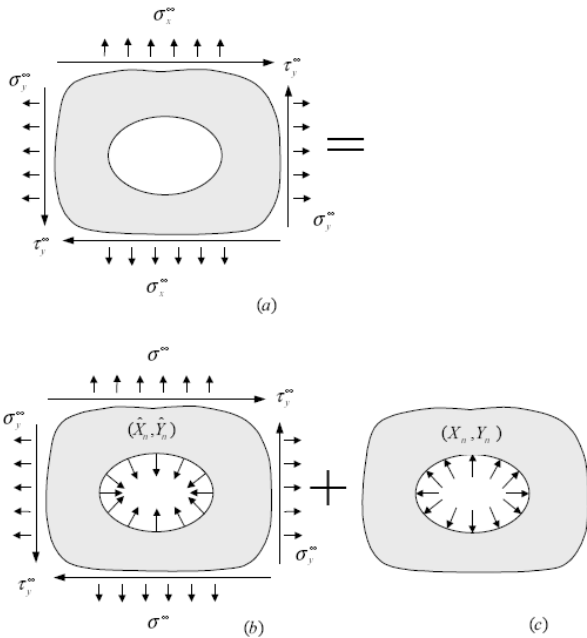


Fig. 3. Analysis case divided into two separate cases [4]

In the case 3c, the additional loading is defined as:

$$\begin{aligned} X_n &= \sigma_x^\infty \cos \delta + \tau_{xy}^\infty \sin \delta \\ Y_n &= \tau_{xy}^\infty \cos \delta + \sigma_y^\infty \sin \delta \end{aligned} \quad (4)$$

The derivation of the stress components is based on Airy's stress function and complex potentials. The solution depends on the roots of the characteristic equation. The case with pairwise equal roots is a special case and it is not covered in this paper. In typical laminates the roots are different. The characteristic equation is defined as:

$$\begin{aligned} a_{11}\mu^4 - 2a_{16}\mu^3 + (2a_{12} + a_{66})\mu^2 \\ - 2a_{26}\mu + a_{22} = 0 \end{aligned} \quad (5)$$

The principal complex roots of the characteristic equation are denoted as μ_1 and μ_2 . The stress state in the laminate is obtained from equations:

$$\sigma_x = \text{Re} \left(\frac{g_2 f_1 \mu_1^2 - g_1 f_2 \mu_2^2}{\mu_1 - \mu_2} \right) \quad (6)$$

$$\sigma_y = \text{Re} \left(\frac{g_2 f_1 - g_1 f_2}{\mu_1 - \mu_2} \right) \quad (7)$$

$$\tau_{xy} = \text{Re} \left(\frac{g_2 f_1 \mu_1 - g_1 f_2 \mu_2}{\mu_1 - \mu_2} \right) \quad (8)$$

where the terms g and f are defined as follows:

$$g_1 = i\lambda\sigma_x^\infty - \mu_1\sigma_y^\infty - (1 - i\mu_1\lambda)\tau_{xy}^\infty \quad (9)$$

$$g_2 = i\lambda\sigma_x^\infty - \mu_2\sigma_y^\infty - (1 - i\mu_2\lambda)\tau_{xy}^\infty \quad (10)$$

$$f_1 = \frac{1 - i\mu_1\lambda}{\beta_1 \sqrt{\beta_1^2 - 1 - \mu_1^2 \lambda^2} \pm (\beta_1^2 - 1 - \mu_1^2 \lambda^2)} \quad (11)$$

$$f_2 = \frac{1 - i\mu_2\lambda}{\beta_2 \sqrt{\beta_2^2 - 1 - \mu_2^2 \lambda^2} \pm (\beta_2^2 - 1 - \mu_2^2 \lambda^2)} \quad (12)$$

where $\lambda = b/a$. In addition the terms β are defined as follows:

$$\beta_1 = \frac{r}{a}(\cos \psi + \mu_1 \sin \psi) + \frac{d}{a}(\cos \delta + \mu_1 \sin \delta) \quad (13)$$

$$\beta_2 = \frac{r}{a}(\cos \psi + \mu_2 \sin \psi) + \frac{d}{a}(\cos \delta + \mu_2 \sin \delta) \quad (14)$$

Under certain conditions the negative forms in terms f_1 and f_2 should be used. The conditions depend on laminate lay-up, angle ψ and distance d .

After solving the laminate stress state the analysis method is the same as before. The average stress within characteristic distance is obtained from:

$$\{\bar{\sigma}\}_{xy} = \frac{1}{d_0} \int_0^{d_0} \{\sigma\}_{xy} dn \quad (15)$$

and ply stresses in critical ply obtained from:

$$\{\sigma_{ply}\}_{12} = [T]\{\bar{Q}\}[a^*]\{\bar{\sigma}\}_{xy} \quad (16)$$

where $[T]$ is the coordinate transform matrix, $\{\bar{Q}\}$ is the ply stiffness matrix in xy -coordinate system and $[a^*]$ is the normalized stiffness matrix of the laminate.

2.3 Failure Criteria

The previous analysis method was based on the maximum stress criterion and the failure of 0° plies. This was found to work well with typical laminate lay-ups in uniaxial loading. With new analysis method also other failure criteria are possible to use. This is necessary especially with laminates that does not include any 0° plies.

The failure criteria used in this study are maximum stress, Tsai-Hill, Tsai-Wu and Hoffmann. The maximum stress criterion is used in order to compare the results with previous analysis method. Other criteria are fully interactive in order to account for multiaxial stress state in the ply. Partially interactive failure criteria, such as Puck or Hashin, are not used in this study because in compression loading the equation estimating the

fiber fracture simplifies to maximum stress criterion.

2.4 Finite Width Correction Factor

In the previous analysis method the finite width correction factor developed for isotropic materials was used. In this paper the factor developed for orthotropic materials was also used but the difference to the isotropic factor was found to be negligible with the laminates under study.

The finite width correction factors found from the literature use the ratio between ellipse semi-axes λ . In this study the coordinate system is different and instead of λ , its inverse value must be used. The ϑ is defined as:

$$\vartheta = \frac{a}{b} = \frac{1}{\lambda} \quad (17)$$

The finite width correction factor for isotropic materials is then

$$Y_3 = \frac{1}{(1 - \vartheta^2)} + \frac{1 - 2\vartheta}{(1 - \vartheta)^2} \sqrt{1 + (\vartheta^2 - 1) \left(\frac{2b}{W} M\right)^2} - \frac{\vartheta^2}{1 - \vartheta} \left(\frac{2b}{W} M\right)^2 \left[1 + (\vartheta^2 - 1) \left(\frac{2b}{W} M\right)^2 \right]^{-1/2} \quad (18)$$

where

$$M^2 = \frac{\sqrt{1 - 8 \left[\frac{3 \left(1 - \frac{2b}{W}\right)}{2 + \left(1 - \frac{2b}{W}\right)^3} - 1 \right]} - 1}{2 \left(\frac{2b}{W}\right)^2} \quad (19)$$

For orthotropic materials the finite width correction factor is more complicated:

$$Y_4 = \frac{\vartheta^2}{(1-\vartheta^2)} + \frac{1-2\vartheta}{(1-\vartheta^2)^2} \sqrt{1 + (\vartheta^2 - 1) \left(\frac{2b}{W} M\right)^2} - \frac{\vartheta^2}{1-\vartheta} \left(\frac{2b}{W} M\right)^2 \left[1 + (\vartheta^2 - 1) \left(\frac{2b}{W} M\right)^2 \right]^{-1/2} + \frac{\vartheta^7}{2} \left(\frac{2b}{W} M\right)^6 \left(K_t - 1 - \frac{2}{\vartheta}\right) \left[\left(1 + (\vartheta^2 - 1) \left(\frac{2b}{W} M\right)^2\right)^{-5/2} - \left(\frac{2b}{W} M\right)^2 \left(1 + (\vartheta^2 - 1) \left(\frac{2b}{W} M\right)^2\right)^{-7/2} \right] \quad (20)$$

where

$$K_t = \frac{1}{1 + \frac{1}{\vartheta} \sqrt{\frac{2}{A_{66}} \left(\sqrt{A_{11}A_{22}} - A_{12} + \left(\frac{A_{11}A_{22} - A_{12}^2}{2A_{66}} \right) \right)}} \quad (21)$$

2.5 Characteristic Length

The characteristic length denoted in this paper as d_0 is kept the same as in the previous study and is considered as material constant because that was one of the main conclusions in original work [1-2]. The previous method was based on observation that the change in characteristic distance with different laminates was small enough in order to consider it as a constant value.

It must be kept in mind that using the characteristic distance defined in the previous study was based on maximum stress criterion alone. Therefore, the value obtained from that work is not necessarily similarly applicable for other failure criteria.

3 Test Arrangements

All tests performed in this study are based on compression after impact (CAI) test standard AITM 1.0010 [7]. The version used was issue 2.

3.1 Test Specimens

The specimen dimensions are 100×150 mm. All specimens had 24 plies resulting to nominal thickness of 3.4 mm.

Total number of five different lay-ups was used in the tests. Two of the lay-ups had no plies in the 0° direction. The laminate lay-ups used in the tests are presented in Table 1.

Table 1. Laminate lay-ups used in the tests

Code	Lay-up
Lam1	[4(0/60/-60/-60/60/0)]
Lam2	[45/-45/0/45/-45/90/45/-45/0/45/-45/90]se
Lam3	[0/45/-45/0/45/-45/0/45/-45/0/90/0]se
Lam4	[3(-45/30/-30/45/45/-30/30/-45)]
Lam5	[6(30/-30/-30/30)]

The impact energies used in the tests were the same as in the previous study i.e. 10J and 14J. The laminate lay-ups 1-3 were impacted with 10J, lay-up 5 with 14 J and lay-up 4 with both 10J and 14J.

The specimens were manufactured from AS4/3501-6 carbon/epoxy prepreg. Laminates were laid onto flat aluminum mold. Debulking was performed after three layers. The panels were cured in an autoclave. The cure temperature was 180 °C and the curing time was 2 hours. The cure cycle included a dwell period of 1 hour at 120 °C. The dimensions of the manufactured panels were 340×340 mm.

The test specimens were machined from the panels using a circular saw. All edges were made smooth with sandpaper.

3.2 Test Equipment

The impact tests were performed using a drop weight impact testing machine. The machine is equipped with a catcher that prevents multiple impacts on the specimen.

The mass of the impactor was 1.702 kg and the drop heights were 0.599 m and 0.837 m for 10J and 14J impact energies respectively. The impactor head was a hemispherical with 16 mm diameter.

The compression load was applied to the specimens using a hydraulic uniaxial testing machine with the maximum loading capacity of 100 kN. A compression after impact test fixture

preventing the specimen global buckling was used in the tests.

3.3 Inspection of Specimens

All specimens were inspected with ultrasonic NDI equipment before and after impact tests. The NDI equipment used was Olympus Omniscan MX phased array ultrasonic scanner. The probe was Olympus 5L64-NW1 which has 64 elements with 5 MHz frequency.

The specimens were immersed in water tank during inspection. The tank was equipped with Olympus Glider encoding scanner for measurement of dimensions. The analysis of inspection results was made with Tomoview software and the size of the damage was defined with -6dB criterion from the C-scan image. The equipment used in specimen inspections is presented in Fig. 4 and an example of C-scan image is presented in Fig. 5.



Fig. 4. Ultrasonic NDI equipment (left) and water tank with xy-scanner (right)

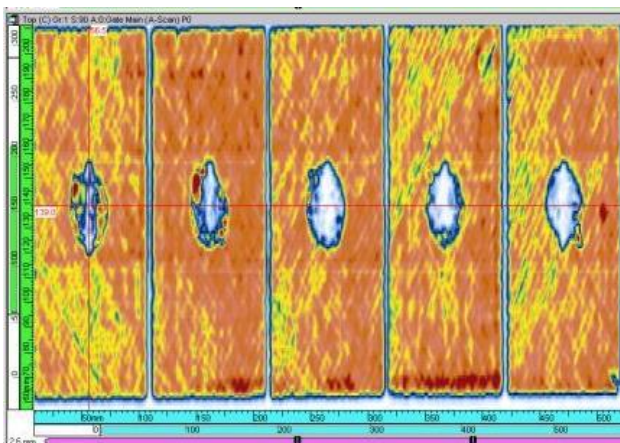


Fig. 5. An example of C-scan image

3.4 Test Matrix

The test matrix is shown in Table 2. The test matrix presents the number of specimens for

different laminate lay-ups and impact energies used in the test program.

Table 2. The test matrix

Series	Laminate	Energy	Specimens
1.1	Lam1	10J	5
2.4	Lam2	10J	5
3.6	Lam3	10J	5
a	Lam4	10J	6
b	Lam5	14J	6
c	Lam4	14J	6

4 Test Results

The results from the ultrasonic inspection of impact damages are presented in Table 3 together with measured dent depths. The table presents the average width and average dent depth of the damage.

Table 3. The measured damage characteristics.

Series	Impact	Damage width [mm]	Dent depth [mm]
1.1	10J	31.4	0.13
2.4	10J	32.2	0.08
3.6	10J	27.1	0.19
a	10J	27.6	0.20
b	14J	24.6	0.48
c	14J	30.9	0.30

The measured damage sizes are of same order of magnitude although different impact energies and laminate lay-ups are used. In dent depths more variation can be found. Also, the difference between lay-ups impacted with same energy is clearly visible.

The CAI test results are presented in Table 4. The table presents the average failure stresses together with standard deviation.

Table 4. Compression after impact test results.

Series	Failure Stress [MPa]	Deviation	
		[MPa]	%
1.1	178.32	19.44	10.9
2.4	163.71	9.78	6.0
3.6	222.77	32.04	14.4
a	181.47	1.57	0.9
b	164.93	18.94	11.5
c	172.30	3.20	1.9

In test series a and c the deviation in the results is very small. In other tests the deviation is reasonable and typically only one specimen in each series differs from others.

The failure of compressed test specimens is presented in Fig. 6. The outmost plies are buckled through the width. The failure mode is typical for all test specimens except those in test series b. The failure mode of specimens in test series b is presented in Fig. 6. (right) The outmost plies are again buckled but the area is more localized to the center of the specimen than in other test series. In addition, shear failure of top plies is also visible.

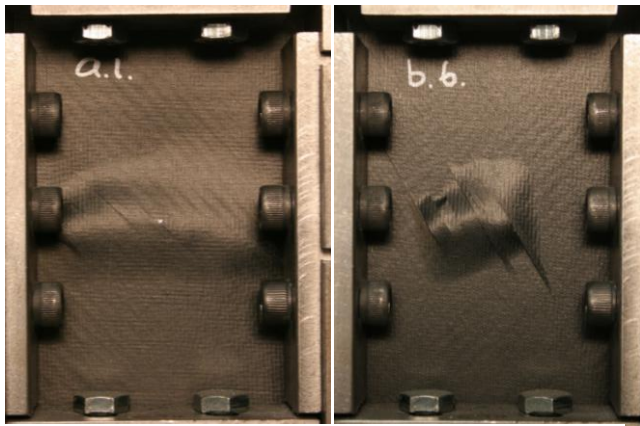


Fig. 6. Typical failure of specimens (left) and failure of ±30 –type laminate (right)

In addition to the test results presented in this study the notched laminate tests performed during the previous study are used to evaluate the analysis method. The test results are presented in [3].

The laminate lay-ups used in the notched laminate tests were quasi-isotropic with two different ply orientations: 1) [3(0/45/-45/90/90/-45/45/0)] and 2) [4(0/60/-60/-60/60/0)]. Both laminates had total amount of 24 plies and the nominal thickness of the laminate was 3.4 mm. The notch geometries used in the tests were round and elliptical. The dimensions the notch geometries are presented in Table 5. More details about the notched laminate tests can be found in [3].

Table 5. Notch geometries used in tests

Notch	Width [mm]	Height {mm]	Width/height
P1	25	25	1
P2	36	36	1
E1	25	12.5	2
E2	36	12	3

5 Analysis vs. Test Results

The characteristic length used in all analyses was $d_0 = 2.426$. In addition, the maximum stress criterion is used only to estimate fiber failure in order to be consistent with previous analyses.

All analyses are performed at $\psi = 90^\circ$ i.e. the same angle as in previous method. Therefore, the results obtained using maximum stress criterion are the same as before and the difference when using other failure criteria is clearly visible.

The analysis results compared to the notched laminate test results are presented in Fig. 7. With quasi-isotropic laminate the results from maximum stress and Tsai-Hill criteria are equal. They also provide lowest estimates on the strength in all cases. The difference is most significant with elliptical holes. Tsai-Wu criterion produces highest estimates for all notch geometries. The results obtained with Tsai-Wu criterion for round holes are between the tested results of the two laminates. The most consistent analysis results for notched laminates are obtained with Hoffmann criterion. The Hoffmann predicts well the test results from round holes and slightly underestimates the results from elliptical holes.

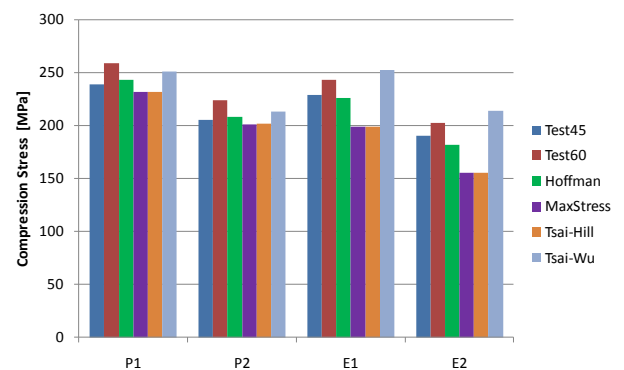


Fig. 7. Test results vs. analyses for notched laminates

The analysis results compared with impact damaged laminates are presented in Figs. 8-13. The analysis is based on equivalent elliptical hole where the width of the ellipse is the same as width of the actual impact damage. The height of the equivalent hole is obtained from the height of the dent.

The Fig 8 presents the results compared to quasi-isotropic laminate. In this case the closest estimates are obtained with maximum stress and Tsai-Hill criteria. The Hoffmann criterion overestimates the tests results by 15% and Tsai-Wu 44% respectively.

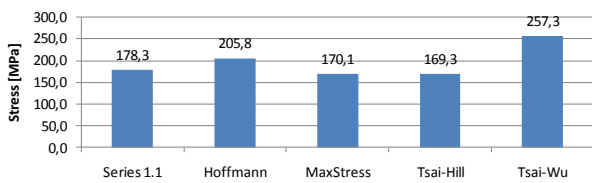


Fig. 8. Test results vs. analysis results for lam1, 10J

The Fig 9 presents analysis and test results obtained for lam2 lay-up which is $\pm 45^\circ$ dominated laminate. The behavior of results is similar as in quasi-isotropic laminate. Maximum stress and Tsai-Hill results are nearly equal and lower than test results (-9%), whereas Hoffmann results overestimate the test results by 6%. Tsai-Wu results are clearly overestimated by 25%.

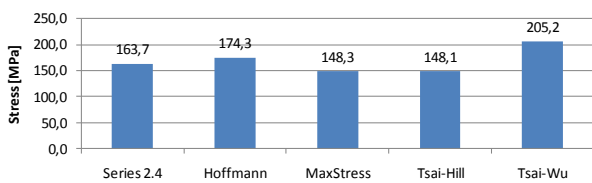


Fig. 9. Test results vs. analysis results for lam2, 10J.

The Fig 10 presents analysis results vs. test results for lam3 lay-up which is 0° dominated laminate. In this case all failure criteria overestimate the tested value. Closest estimates are obtained from maximum stress and Tsai-Hill criteria (11%) while Hoffmann overestimates by 36% and Tsai-Wu by 72%.

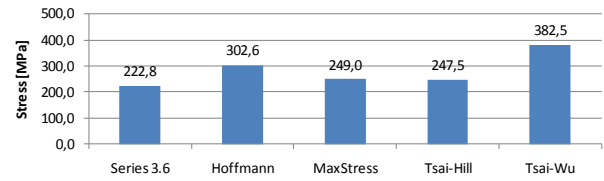


Fig. 10. Test results vs. analysis results for lam3, 10J

In the analysis point of view most interesting test results are obtained from laminates that include no 0° plies. In these cases all layers are in multiaxial stress state although the external loading is uniaxial.

The comparison between test results and analysis for $\pm 30/\pm 45$ -type laminate with 10J impact damage is presented in Fig. 11. In this case the maximum stress criterion clearly overestimates the tested value by 34%. Results from Tsai-Hill criterion differ now significantly from maximum stress results underestimating the tested value only by 12%. Other results are very close to the tested value, Hoffmann -6% and Tsai-Wu -1%.

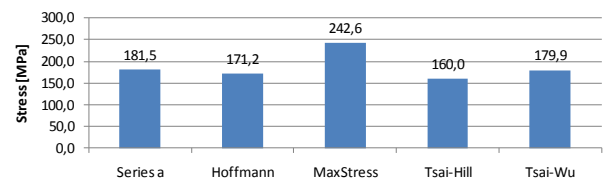


Fig. 11. Test results vs. analysis results for lam4, 10J

For ± 30 -type laminate the error in maximum stress results are even worse: it overestimates the tested result by 139%. The results are presented in Fig. 12. It must be kept in mind that the maximum stress result is calculated with respect to fiber fracture as it was assumed in the previous analysis method. For other failure modes the estimate would be closer to the tested value.

It is also notable that for this type of laminate the Tsai-Hill now overestimates the tested value by 18%. Other two results are again very close to the tested value: Hoffmann 1.2% and Tsai-Wu -1.5%.

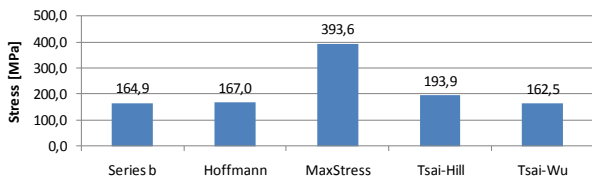


Fig. 12. Test results vs. analysis results for lam5, 14J

The Fig. 13 presents the analysis results vs. test results for the $\pm 30/\pm 45$ -type laminate with 14J impact damage. The results are consistent with the results obtained with 10J impact. The error in percentages is very similar to those obtained with 10J impact.

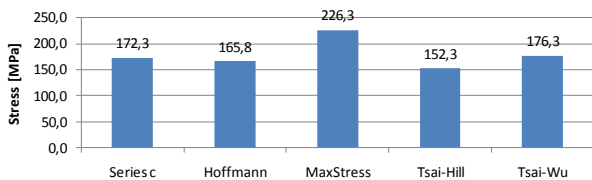


Fig. 13. Test results vs. analysis results for lam4, 14J

6 Conclusions

Based on the work performed the following conclusions can be made

- The new analysis method presented in this paper is based on complex potentials as the previous method. The equations used are the same as in ESAComp software but the method is extended to use average stresses instead of point stresses.
- The test series performed were successful providing additional reference strength data for different types of laminates.
- The analysis of balanced laminates without 0° plies shows clearly the flaws with the previous analysis method based on maximum stress criterion. With the new analysis method it is possible to take into account the multiaxial stresses at arbitrary angle along the hole edge.
- The purpose of this study was not to evaluate the superiority of failure criteria. The analysis results are possible to fit better with the test results if the characteristic length is defined for all failure criteria separately.

- In order to reliably define the characteristic length a test series of notched laminates with different lay-ups including symmetric and balanced laminate without 0° is needed. The geometry of notch is clearly defined and therefore the only open parameter left in the analysis is the characteristic length.
- The test program using notched laminates and balanced lay-ups without 0° plies would provide also information about the correct location of failure around the hole edge.
- The analysis method used in this study is a very useful tool for estimating compression loaded laminates with various lay-ups. It is possible to extend the method to cover also multiaxial external load cases.

Acknowledgements

The research described in this paper was carried out at Aalto University, School of Science and Technology, Department of Applied Mechanics under a contract with the Finnish Air Force.

References

- [1] Chen P., Shen Z., Wang J.Y., Prediction of the Strength of Notched Fiber-Dominated Composite Laminates. *Composite Science and Technology*, vol 61, 2001, Elsevier Science Ltd. 1311-1321.
- [2] Chen P., Shen Z., Wang J.Y., A New Method for Compression After Impact Strength Prediction of Composite Laminates. *Journal of Composite Material*, vol 36, No. 5/2002. Sage Publications. 589-610.
- [3] Wallin M., Saarela O., Compression Strength of the Notched and Impact Damaged Composite Laminates. *26th International Congress of the Aeronautical Sciences*, 14-19 September 2008, Anchorage, Alaska USA. 9 pages.
- [4] Yuejin L., Palanterä M., Notched Laminates, *Theoretical Background of the ESAComp Analyses*, version 1.5, 14.4.1999, 16 pages
- [5] Lekhnitskii S.G., *Anisotropic Plates*, Gordon and Breach Science Publishers, New York, 1968. 534 p.
- [6] Tan S.C., *Stress Concentrations in Laminated Composites*. Lancaster Technomic, 1994.
- [7] Determination of Compression Strength after Impact, *Airbus Industrie Test Method, Fiber Reinforced Plastics, AITM 1.0010*, Issue 2, June 1994, 11 p.

Copyright Statement

The authors confirm that they, and/or their company or organization, hold copyright on all of the original material included in this paper. The authors also confirm that they have obtained permission, from the copyright holder of any third party material included in this paper, to publish it as part of their paper. The authors confirm that they give permission, or have obtained permission from the copyright holder of this paper, for the publication and distribution of this paper as part of the ICAS2010 proceedings or as individual off-prints from the proceedings.